Carbon Nanotube Conductive Additives for Improved Electrical and Mechanical Properties of Flexible Battery Electrodes

Sarah Jessl[1], David Beesley[1], Simon Engelke[1,2], Christopher J. Valentine[1], Joe C. Stallard[3], Norman Fleck[3], Shahab Ahmad[1], Matthew T. Cole[4], Michael De Volder[1,*]

[1] University of Cambridge, Department of Engineering, Institute for Manufacturing, Cambridge CB2 1PZ, United Kingdom

[2] University of Cambridge, Cambridge Graphene Centre, Cambridge, CB3 0FA, United Kingdom

[3] University of Cambridge, Department of Engineering, Cambridge Centre for Micromechanics, Cambridge CB2 1PZ, United Kingdom

[4] University of Bath, Department of Electronic & Electrical Engineering, Claverton Down, Bath BA2 7AY, United Kingdom

* E-mail: mfld2@cam.ac.uk

Keywords: Carbon Nanotubes, flexible electrodes, flexible batteries, conductive additives, resistance measurements

Abstract:

Flexible electronics are being pursued as replacements for rigid consumer electronic products such as smartphones and tablets, as well as for wearable electronics, implantable medical devices, and RFIDs. Such devices require flexible batteries with electrodes that maintain their electro-chemical performance during multiple bending cycles. These electrodes typically consist of an active battery material blend with a conductive additive and a binder. Whilst the choice of active battery material is typically dictated by the desired battery power and energy requirements, there is more freedom in changing the conductive additives to cope with strain induced during the bending of flexible batteries. Here we compare the mechanical and electrical properties of free standing cathodes using lithium cobalt oxide ($LiCoO_2$) as the active material and 10 to 20 wt% of amorphous carbon powder (CP) or carbon nanotubes (CNTs) as conductive additives. We found that the CNT based electrodes showed less crack formation during bending and have a Young's modulus up to 30 times higher than CP electrodes (10 wt%

loading). Further, the electrical resistance of pristine CNT electrodes is 10 times lower than CP electrodes (20 wt% loading). This difference further increases to a 28 times lower resistance for CNT films after 2000 bending cycles. These superior properties of CNT films are reflected in the electrochemical tests, which show that after bending, only the electrodes with 20 wt% of CNTs remain operational. This study therefore highlights the importance of the conductive additives for developing reliable flexible batteries.

Introduction:

Over the past decade, substantial progress has been made in the fabrication of flexible electronic devices such as roll-up displays, wearable electronics, active radio frequency identification (RFID) tags, as well as implantable biomedical devices [1]–[8]. As these devices move closer towards commercialization, it is becoming increasingly important to develop suitable flexible and stretchable energy storage devices. As lithium-ion battery technology currently holds the most promise for achieving the energy and power density required for these applications [9], [10], it is crucial to understand the impact of mechanical stress due to bending on the electrodes and how to improve their flexibility. This is, however, a challenging task since the degradation in battery performance can be due to delamination between the electrode film and current collector; loss of physical contact between particles; formation of cracks in the electrodes; etc [11]. For flexible batteries using classic conductive additives (e.g. Super-P carbon) several reports have looked into the electrical and mechanical properties, the adhesion to the collector electrode, and in particular the influence of the polymer-binder on these properties [12][13][14][15][16] [37] [38] [46].

Several strategies have been proposed to improve the flexibility of batteries.[11], [17]–[20] For instance, decreasing the thickness of the battery electrode layers [21], structuring or patterning the collector electrode [22], or embedding the active material in porous substrates [23], fabrics

[24], paper [25], or plastic [11],[12] have been reported to enhance flexibility and robustness. However, most of these solutions rely on non-conductive flexible support materials such as paper and plastic, which decrease the volumetric performance, and often reduce the electrical conductivity or react with the electrolyte. Therefore, flexible and conductive support materials, such as carbon powder [28], graphene or reduced graphene oxide [29]–[31] and carbon nanotubes (CNTs) are attractive alternatives [32]–[36].

This work investigates CNTs as a replacement for standard carbon black Super-P powder (CP) as a conductive additive because of their excellent electrochemical stability and good mechanical and electrical properties [39], [40]. The addition of CNTs as a conductive additive has been shown to increase the conductivity of the electrode [41], [42], and because of their high aspect ratio 1D structure, they are believed to form a network that mechanically binds the active material together, which mitigates crack formation during bending [43] and provides high strength [44]. Whilst the electrical conductivity of CNT-active material composites has been reported previously [45], the effect of bending the film on the resistance for different compositions of those films has to the best of our knowledge not been shown before. Here we show how that the type of conductive additive can have a very large influence on the conductivity of flexibility during bending. For instance, the initial resistance of an electrode with 20 wt% CNT conductive additive was 61 Ω, and increases to 67 Ω after 2000 bending cycles, whereas 20 wt% CP film starts at 640 Ω and increases to as much as 1883 Ω after the same bending cycles. Further, mechanical tests show the CNT based films can have Young's moduli up to 30 times higher than those of CP based films, and after 2000 bending cycles, the CNT based films did not show any cracks, whereas these are clearly apparent in CP based films under the same bending conditions. Overall, the CNT based batteries outperformed CP based ones, which shows the importance of the conductive additives for flexible battery electrodes.

Methods

We used lithium cobalt oxide (LCO) cathodes as a model system in this paper. The electrodes are made by sonicating a mixture of LCO, PVDF and CNTs or CP for 1 hour in N-Methyl-2-pyrrolidon (NMP) followed by ball milling for 2 hours (see experimental section). Then the films are cast onto glass slides or on Aluminum foil, dried, and peeled off from their supports. The electrodes are then cut to size for stress-strain measurements, electrical measurements, and battery testing. For the latter, the films are cut into discs (4.76 mm in diameter) to increase the ratio of affected area by bending. The electrochemical properties of the compounds are evaluated in 2032 coin cells against lithium metal foils (half-cells). 1.0 M LiPF6 EC/EMC=50/50 (v/v) electrolyte and Celgard separators are used in the coin cells. Depending on the measurements, the electrodes were bent 100 to 2000 times (see experimental section).

Results and Discussion

Figure 1 shows SEM images of the films before and after bending for 10 wt% of CNTs (CNT10, Figure 1A), 10 wt% of CP (CP10, Figure 1B) and 20 wt% of CP (CP20, Figure 1C). The smooth surface of the CP films compared to the CNT film suggests the CP particles are better mixed in the electrode during ball milling. CNT bundles are visible in the inset SEM image of Figure 1A, whereas small particles can be seen in the inset of Figure 1B. After bending the electrodes, 2000 times at a bend radius of 3 mm, the CNT10 film does not show any cracks at all. Some cracks were already observed in the CP10 film after only 100 bends, whilst the CP20 films show cracks after 2000 bending cycles. Hence, the CNT10 films are found to be stable during bending. The SEMs for the films with 20 wt% CNTs also show no change and can be found in **Figure S1**. The absence of cracks in the CNT based electrodes suggests that the CNTs form an interconnected network that mechanically binds the active material as depicted in the schematics of Figure 1A. A close-up SEM image of this CNT network in a 10 wt% electrode is shown in **Figure S2**.

Next, the stress-strain curves of electrodes with 10 wt% and 20 wt% CP or CNT additive were measured using the test setup depicted in **Figure 2A**. As shown in Figure 2B, the CNT electrodes are stiffer than the CP electrodes, with the CNT20 nearly double the stiffness compared to the CNT10 (see **Figure 2B** and force-strain curves in **Figure S3**). The Young's Modulus for CNT20 is 1.3 GPa, CNT10 is 0.70 GPa and CP10 is 0.023 GPa. The 20 wt% CP electrodes were too brittle to be measured in the present setup, which clearly illustrates the influence of the CNTs on the mechanical properties of the films.

Next, the electrical conductivity of the electrodes is investigated during bending. The change in resistance of the four electrodes as a function of the bending angle as well as during repeated bending (2000 cycles, bending radius 3 mm) is monitored. For this, we used a custom-built bending rig.[47] To best of our knowledge, such in-situ measurements of the resistance of the electrode during bending have not been reported before. As shown in **Figure 3A**, the initial resistance of electrode films using CNTs is lower than that of CP films (see **Table 1**). Further, the increase in resistance for both CP films (10% and 20%) is significantly higher than for the CNT films, for instance 20 wt% CNT films only increase by 10% in resistance, (close-up view of graph can be found in **Figure S4**) while the resistance of 20 wt% CP films increases by 194%. As mentioned above, we attribute these findings to the interconnected network of CNTs around the active material which is more robust, as well as remaining conformal during bending compared to the physical connections formed by the spherical CP-particles. It is important to note that the overall resistance of the CNT films is already 50% lower prior to bending, making it a more attractive carbon additive for flexible battery electrodes. **Figure 3B** and **3C** show the change in resistance for the films with varying bending angles during the first bending cycle (Figure 3B) and after 2000 bending cycles (Figure 3C). During the first bending cycle, the 20 wt% CP film increases by 47% in electrical resistance while the 20 wt% CNT film increased

by only 4% (Figure 3B). After 2000 bending cycles (Figure 3C), the difference in resistance is stable during bending, indicating that a steady state condition is reached. A direct comparison for each type of film can be found in **Figure S6**.

The impact of mechanical bending on the performance of batteries using CP and CNTs as conductive additives is investigated in the following section. First the LCO powder (Sigma Aldrich) is characterized via XRD (**Figure 4A**) and then tested using cyclic voltammetry (Figure 4B), which both show the expected LCO peaks. Next, the freestanding electrodes are tested in half-cell configuration, for which 24 coin cells have been assembled with at least 4 cells of each formulation. Half of the electrodes are bent once or twice, while the other half were bent 100 times to a bending radius of 3 mm before being inserted into the coin cells (see experimental section). Of the 24 cells tested, only the cells with 20 wt% CNT electrodes are operational which is in agreement with the poor electrical conductivity measured in the other electrode formulations (see Table 1) as well as the cracks observed in CP batteries after bending. Additionally, the 20 wt% CNT electrodes may have a better porosity which helps the diffusion of Li-Ions. Figure 4C shows the initial capacities of 20 wt% CNT electrodes (bent once compared to bent 100x). The slightly lower capacity of the 100x bent electrode might be due to local delamination of the electrode. Finally, Figure 4D shows repeated charge-discharge curves of a bent 20 wt% CNT electrode showing a good charge retention. This improvement in electrochemical performance is in agreement with the enhanced electrical and mechanical properties measured in the CNT based electrodes. With the increase in production volumes of CNTs [39], we anticipate that this will become a viable solution, in particular as an additive for cathodes where high the surface area of the CNTs does not lead to as many side reactions as on the anode side.

Conclusion

This paper shows that the use of CNTs instead of CP as conductive additives in a conventional electrode formulation significantly improves the mechanical and electrical performance during multiple bending cycles. We found that for equal mass loading, the CNT electrodes have a higher Young's Modulus and less crack formation, as well as much lower electrical resistance (10 times lower for 20 wt% CNTs compared to 20 wt% CP). Further, we studied the evolution of the electrical conductivity over thousands of bending cycles for the first time and found that the electrical resistance of CNT films increased significantly less than the conventional CP films. After 2000 bending cycles, the resistance of 20 wt% CNT film is 28 times lower than 20 wt% CP film, which suggests that CNTs are particularly interesting for flexible battery electrodes. This was reflected in the electrochemical performance of bent electrodes, where we found that only the films with 20 wt% CNTs were operational.

Acknowledgements

S.J., S.A. and M.D.V. acknowledge ERC starting grant 337739-HIENA. S. E. acknowledges funding from EPSRC grant EP/L016087/1 Graphene CDT. C.J.V. acknowledges the Engineering and Physical Sciences Research Council (EPSRC) Sensor CDT (EP/L015889/1). M.T.C. thanks the Oppenheimer Trust and Bath University for generous financial support.

Experimental Section

Casting films from solutions: The films are made by sonicating a mixture of 200 mg lithium cobalt oxide (LCO, Sigma Aldrich), 25 mg CNTs or carbon powder (SuperP, Alfa Aesar) and 25 mg poly(vinylidene fluorid) (PVDF, Sigma Aldrich) for 1 hour in N-Methyl-2-pyrrolidon (NMP, Acros Organics) and ball milling for 2 hours for the 10 wt% conductive additive, 175

mg LCO, 50 mg CNT/ Carbon powder and 25 mg PVDF for the 20 wt% conductive additive films. These are then cast onto the glass slides (for the stress-strain testing) or on Aluminum foil (for the battery testing) and dried in a vacuum oven or on a hotplate at 60 ºC overnight. After that they are peeled off from their supports.

Stress-strain measurements: Test specimens of the desired dimensions are created by taking the films, positioning them between two sheets of paper, and then cutting out samples of measured dimensions with a craft knife. They are then weighed with a microbalance. Thickness measurements are taken at four equally spaced points along the sample length, using a digital micrometer.

The nominal stress is measured in line with the film's longest dimension, using a screw-driven displacement-controlled tensile testing machine, fitted with a 10 N load cell. Stress is applied to the samples through paper tabs, which are bonded to the samples with contact adhesive. Strain is measured within the gauge length by tracking the movement of dots of white acrylic paint applied prior to testing, using a digital camera and image processing software. This method enables strains to be monitored accurately whilst not interfering with the mechanical behavior of the sample. A schematic of the measurements can be seen in Figure 2A.

Bending of films: Most of the films are bent using an automated, custom-built bending rig. Using a bend radius of 3 mm, the free standing films are clamped and bent 2000 times. During the bending cycles sample resistance is automatically extracted from full-range I-V sweeps measured at the no-bend (0º) and fully bent (90º) scenarios using a Keithley 2400 SMU. For the 100 times bending, the films casts on Aluminum foil are manually bent over a 3 mm bend radius and afterwards peeled off the Al-foil.

Battery measurements: Batteries are assembled from freestanding electrode films. For the measurement of the bent films, the films on the foil are bent 100 times. The films are cut into discs (4.76 mm in diameter) to increase the ratio of affected area by bending. The

electrochemical properties of the compounds are evaluated in 2032 coin cells containing metallic lithium foils as cathodes (half-cells). The electrodes are dried under vacuum at 60 °C for 12 hours. 1.0 M LiPF6 EC/EMC=50/50 (v/v) electrolyte and Celgard separators are used in the coin cells. Cyclic voltammetry and galvanostatic measurements are taken at room temperature with Biologic VMP3 and Lanhe potentiostats/galvanostats. The cells are cycled between 3 to 4.3 V and C-Rates from 0.05 to 0.2 C.

Film characterization: The XRD-system used is a D8- B1- Gen10 Bruker XRD. The software X-Pert Highscore Plus is used for the data evaluation. The SEM measurements are performed with a Leo 1530VP Gemini from Zeiss operating at an accelerating voltage of 8 kV and using the InLens-detector. The working distance is varied between 3-10 mm. Samples are not sputtered with a metal layer.

References

[1] J. W. Lee *et al.*, "Soft, thin skin-mounted power management systems and their use in wireless thermography," *Proc. Natl. Acad. Sci.*, vol. 113, no. 22, pp. 6131–6136, 2016.

[2] W. Gao *et al.*, "Fully integrated wearable sensor arrays for multiplexed in situ perspiration analysis," *Nature*, vol. 529, no. 7587, pp. 509–514, 2016.

[3] J. R. Miller and J. R. Miller, "Valuing Reversible Energy Storage," vol. 1312, no. 2012, 2013.

[4] S. Park and S. Jayaraman, "Smart Textiles: Wearable Electronic Systems," *MRS Bull.*, no. August, pp. 585–591, 2003.

[5] B. S. Shim, W. Chen, C. Doty, C. Xu, and N. A. Kotov, "Smart electronic yarns and wearable fabrics for human biomonitoring made by carbon nanotube coating with polyelectrolytes," *Nano Lett.*, vol. 8, no. 12, pp. 4151–4157, 2008.

[6] K. D. Harris, A. L. Elias, and H. J. Chung, "Flexible electronics under strain: a review of mechanical characterization and durability enhancement strategies," *J. Mater. Sci.*, vol. 51, no. 6, pp. 2771–2805, 2016.

[7] J. A. Rogers, T. Someya, and Y. Huang, "Materials and Mechanics for Stretchable

Electronics," *Science*, vol. 327, no. 5973, pp. 1603–1607, 2010.

[8] W. Liu, M.-S. Song, B. Kong, and Y. Cui, "Flexible and Stretchable Energy Storage: Recent Advances and Future Perspectives," *Adv. Mater.*, vol. 29, no. 1, p. 1603436, 2017.

[9] L. Wen, F. Li, and H.-M. Cheng, "Carbon Nanotubes and Graphene for Flexible Electrochemical Energy Storage: from Materials to Devices," *Adv. Mater.*, vol. 28, no. 22, pp. 4306–4337, 2016.

[10] S. Xu *et al.*, "Stretchable batteries with self-similar serpentine interconnects and integrated wireless recharging systems," *Nat. Commun.*, vol. 4, p. 1543, 2013.

[11] H. Chen, B. W. Lu, Y. Lin, and X. Feng, "Interfacial failure in flexible electronic devices," *IEEE Electron Device Lett.*, vol. 35, no. 1, pp. 132–134, 2014.

[12] G. Liu, H. Zheng, X. Song, and V. S. Battaglia, "Particles and Polymer Binder Interaction: A Controlling Factor in Lithium-Ion Electrode Performance," *J. Electrochem. Soc.*, vol. 159, no. 3, pp. A214–A221, 2012.

[13] J. Chen, J. Liu, Y. Qi, T. Sun, and X. Li, "Unveiling the Roles of Binder in the Mechanical Integrity of Electrodes for Lithium-Ion Batteries," *J. Electrochem. Soc.*, vol. 160, no. 9, pp. A1502–A1509, 2013.

[14] B. Son *et al.*, "Measurement and analysis of adhesion property of lithium-ion battery electrodes with SAICAS," *ACS Appl. Mater. Interfaces*, vol. 6, no. 1, pp. 526–531, 2014.

[15] W. Haselrieder, B. Westphal, H. Bockholt, A. Diener, S. Höft, and A. Kwade, "Measuring the coating adhesion strength of electrodes for lithium-ion batteries," *Int. J. Adhes. Adhes.*, vol. 60, pp. 1–8, 2015.

[16] S. Berg, A. Akturk, M. Kammoun, and H. Ardebili, "Flexible batteries under extreme bending: Interfacial contact pressure and conductance," *Extrem. Mech. Lett.*, vol. 13, pp. 108–115, 2017.

[17] G. Zhou, F. Li, and H.-M. Cheng, "Progress in flexible lithium batteries and future prospects," *Energy Environ. Sci.*, vol. 7, no. 4, pp. 1307–1338, 2014.

[18] L. Dong *et al.*, "Flexible electrodes and supercapacitors for wearable energy storage: a review by category," *J. Mater. Chem. A*, vol. 4, no. 13, pp. 4659–4685, 2016.

[19] Y. Hu and X. Sun, "Flexible rechargeable lithium ion batteries: advances and challenges in materials and process technologies," *J. Mater. Chem. A*, vol. 2, no. 28, p. 10712, 2014.

[20] X. Wang, X. Lu, B. Liu, D. Chen, Y. Tong, and G. Shen, "Flexible energy-storage

devices: Design consideration and recent progress," *Adv. Mater.*, vol. 26, no. 28, pp. 4763–4782, 2014.

[21] M. Koo *et al.*, "Bendable inorganic thin-film battery for fully flexible electronic systems," *Nano Lett.*, vol. 12, no. 9, pp. 4810–4816, 2012.

[22] S. Ahmad, D. Copic, C. George, and M. De Volder, "Hierarchical Assemblies of Carbon Nanotubes for Ultraflexible Li-Ion Batteries," *Adv. Mater.*, vol. 28, no. 31, pp. 6705–6710, 2016.

[23] S. Song *et al.*, "Flexible binder-free metal fibril mat-supported silicon anode for high-performance lithium-ion batteries," *ACS Appl. Mater. Interfaces*, vol. 6, no. 14, pp. 11544–11549, 2014.

[24] A. M. Abdelkader, N. Karim, and C. Vallés, "Highly conductive templated-graphene fabrics for lightweight, flexible and foldable supercapacitors," *Mater. Res. Express*, vol. 4, p. 75602, 2017.

[25] L. Hu *et al.*, "Highly conductive paper for energy-storage devices," *Proc. Natl. Acad. Sci.*, vol. 106, no. 51, pp. 21490–21494, 2009.

[26] H. Nishide and K. Oyaizu, "Toward Flexible Batteries," *Science*, vol. 319, no. February, pp. 737–738, 2008.

[27] L. Nyholm, G. Nyström, A. Mihranyan, and M. Strømme, "Toward flexible polymer and paper-based energy storage devices," *Adv. Mater.*, vol. 23, no. 33, pp. 3751–3769, 2011.

[28] B. Liu *et al.*, "Hierarchical three-dimensional ZnCo 2O 4 nanowire arrays/carbon cloth anodes for a novel class of high-performance flexible lithium-ion batteries," *Nano Lett.*, vol. 12, no. 6, pp. 3005–3011, 2012.

[29] J. Kim, W.-H. Khoh, B.-H. Wee, and J.-D. Hong, "Fabrication of flexible reduced graphene oxide–TiO 2 freestanding films for supercapacitor application," *RSC Adv.*, vol. 5, no. 13, pp. 9904–9911, 2015.

[30] S. Lv, F. Fu, S. Wang, J. Huang, and L. Hu, "Eco-friendly wood-based solid-state flexible supercapacitors from wood transverse section slice and reduced graphene oxide," *Electron. Mater. Lett.*, vol. 11, no. 4, pp. 633–642, 2015.

[31] N. N. Li, Z. Chen, W. Ren, F. Li, and H.-M. H.-M. Cheng, "Flexible graphene-based lithium ion batteries with ultrafast charge and discharge rates," *Proc. Natl. Acad. Sci.*, vol. 109, no. 43, pp. 17360–17365, 2012.

[32] L. Hu, H. Wu, F. La Mantia, Y. Yang, and Y. Cui, "Thin, flexible secondary Li-ion paper batteries," *ACS Nano*, vol. 4, no. 10, pp. 5843–5848, 2010.

[33] J. Chen, Y. Liu, A. I. Minett, C. Lynam, J. Wang, and G. G. Wallace, “Flexible, aligned carbon nanotube/conducting polymer electrodes for a lithium-ion battery,” *Chem. Mater.*, vol. 19, no. 15, pp. 3595–3597, 2007.

[34] J. Wang, L. Li, C. L. Wong, and S. Madhavi, “Flexible single-walled carbon nanotube/polycellulose papers for lithium-ion batteries,” *Nanotechnology*, vol. 23, no. 49, p. 495401, 2012.

[35] D. S. Su and R. Schlögl, “Nanostructured carbon and carbon nanocomposites for electrochemical energy storage applications,” *ChemSusChem*, vol. 3, no. 2, pp. 136–168, 2010.

[36] D. Kong *et al.*, “Encapsulating V 2 O 5 into carbon nanotubes enables the synthesis of flexible high-performance lithium ion batteries,” *Energy Environ. Sci.*, vol. 9, no. 3, pp. 906–911, 2016.

[37] A. M. Gaikwad, A. C. Arias, and D. A. Steingart, “Recent Progress on Printed Flexible Batteries: Mechanical Challenges, Printing Technologies, and Future Prospects,” *Energy Technol.*, vol. 3, no. 4, pp. 305–328, 2015.

[38] A. M. Gaikwad and A. C. Arias, “Understanding the Effects of Electrode Formulation on the Mechanical Strength of Composite Electrodes for Flexible Batteries,” *ACS Appl. Mater. Interfaces*, no. February, p. acsami.6b14719, 2017.

[39] M. F. L. De Volder, S. H. Tawfick, R. H. Baughman, and A. J. Hart, “Carbon nanotubes: present and future commercial applications,” *Science (80-.).*, vol. 339, no. 6119, pp. 535–539, 2013.

[40] B. J. Landi, M. J. Ganter, C. D. Cress, R. a. DiLeo, and R. P. Raffaelle, “Carbon nanotubes for lithium ion batteries,” *Energy Environ. Sci.*, vol. 2, no. 6, p. 638, 2009.

[41] C. Sotowa *et al.*, “The Reinforcing Effect of Combined Carbon Nanotubes and Acetylene Blacks on the Positive Electrode of Lithium-Ion Batteries,” *ChemSusChem*, vol. 1, pp. 911–915, 2008.

[42] L.-F. Cui, L. Hu, J. Wook, and Y. Cui, “Light-Weight Free-Standing Carbon Lithium Ion Batteries,” *ACS Nano*, vol. 4, no. 7, pp. 3671–3678, 2010.

[43] J. Ren *et al.*, “Elastic and Wearable Wire-Shaped Lithium-Ion Battery with High Electrochemical Performance,” *Angew. Chemie Int. Ed.*, vol. 53, no. 30, p. 7958, 2014.

[44] K. Evanoff *et al.*, “Ultra strong silicon-coated carbon nanotube nonwoven fabric as a multifunctional lithium-ion battery anode,” *ACS Nano*, vol. 6, no. 11, pp. 9837–9845, 2012.

[45] C. J. Zhang *et al.*, “Enabling Flexible Heterostructures for Li-Ion Battery Anodes

Based on Nanotube and Liquid-Phase Exfoliated 2D Gallium Chalcogenide Nanosheet Colloidal Solutions," *Small*, vol. 13, no. 34, pp. 1–11, 2017.

[46] Z. Wang, W. Zhang, X. Li, and L. Gao, "Recent progress in flexible energy storage materials for lithium-ion batteries and electrochemical capacitors: A review," *J. Mater. Res.*, no. March, pp. 1–17, 2016.

[47] M. H. Kang *et al.*, "Mechanical Robustness of Graphene on Flexible Transparent Substrates," *ACS Appl. Mater. Interfaces*, vol. 8, no. 34, pp. 22506–22515, 2016.

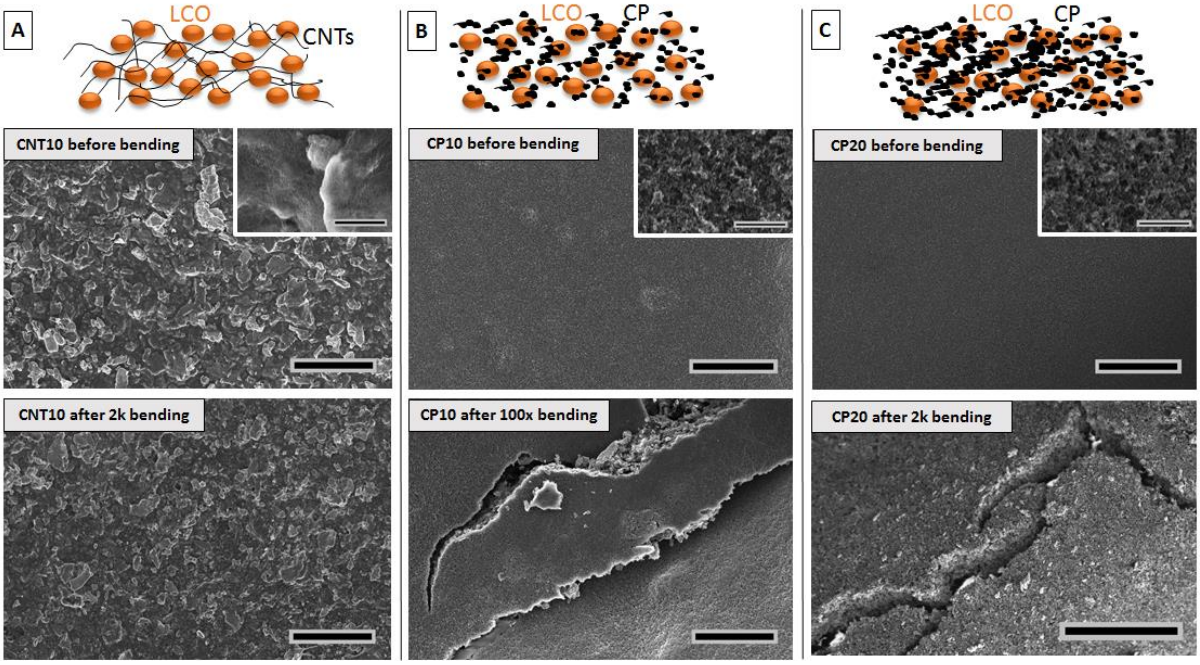

Figure 1: SEM images of the electrodes before and after bending of the films. (A) Mixture of LCO, PVDF and CNTs (80:10:10); (B) Mixture of LCO, PVDF and carbon powder (80:10:10); (C) Mixture of LCO, PVDF and carbon powder (70:10:20). (Scale bar 50 µm, inset 2 µm)

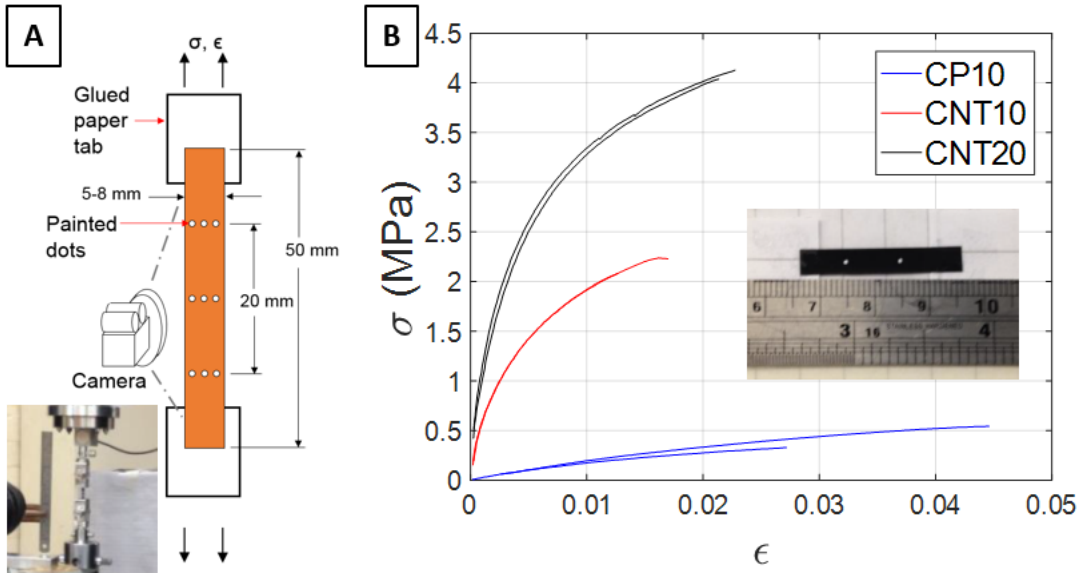

Figure 2: (A) Schematics and photograph of the set-up used for the stress-strain measurements. (B) Stress-strain curves (2 measurements each) for the CNT10, CNT20 and the CP10 films.

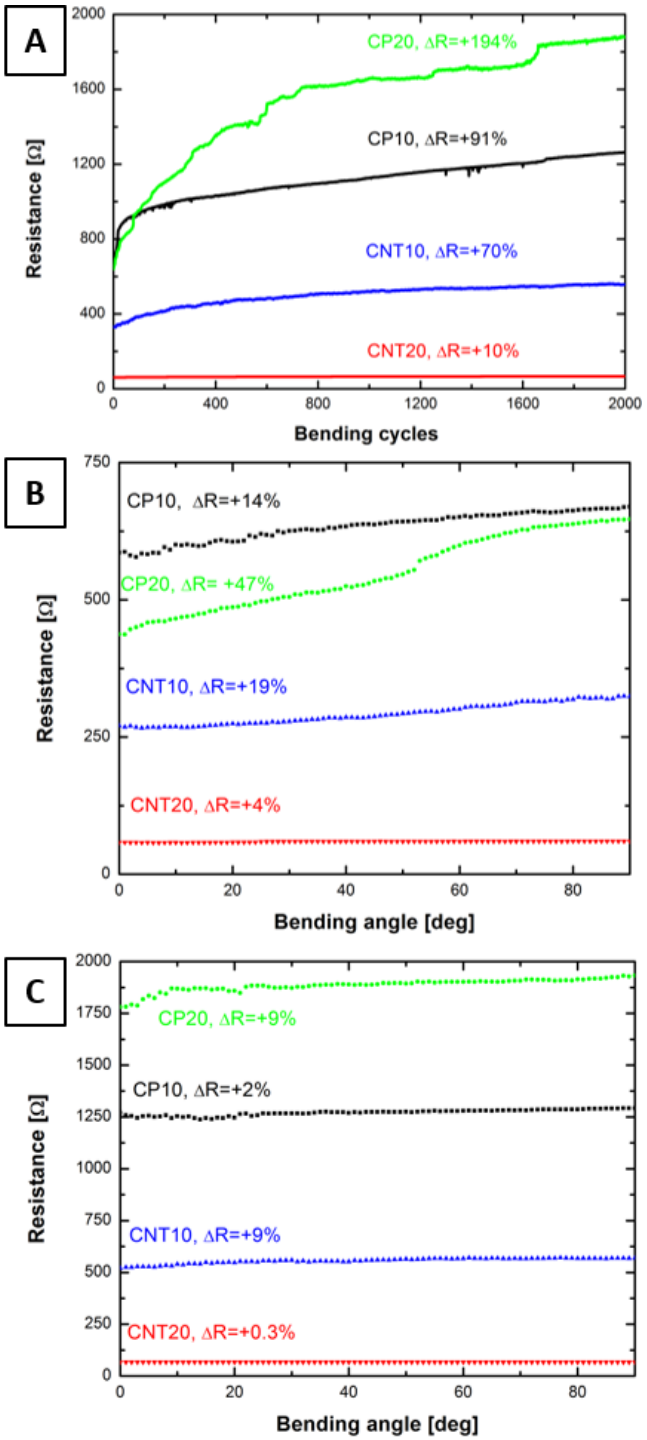

Figure 3: (A) Change in resistance during bending cycles for 10 wt% and 20 wt% CP and CNT as conductive additive. (B,C) Change in resistance as a function of the bending angle of the electrode.

Table 1: Overview of changes in resistance cathodes with different carbon additives.

	CP10	CP20	CNT10	CNT20
Initial resistance [Ω]	660	640	327	61
Resistance after bending	1263	1883	557	67
Percentage change [%]	91	194	70	10

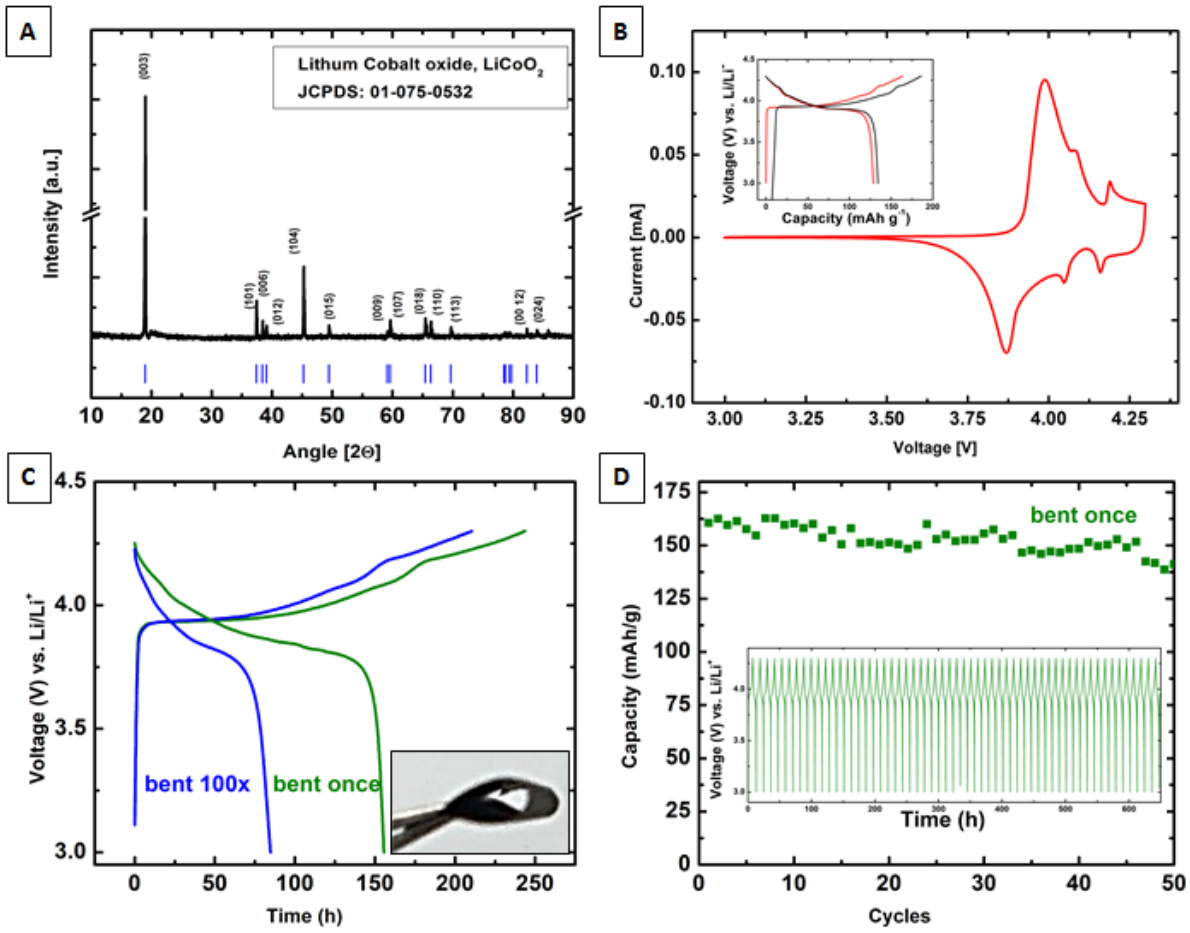

Figure 4: (A) XRD measurement of the LCO powder used in the electrodes along with the JCPDS card; (B) CV curve and charge-discharge curves; (C) Capacity of the second cycle of 20 wt% CNT cathodes bent once (green) and 100 times (blue), inset shows an exemplary bent electrode; (D) Capacity retention during charge-discharge cycles of a 20 wt% CNT film bent once.

Supplementary Information

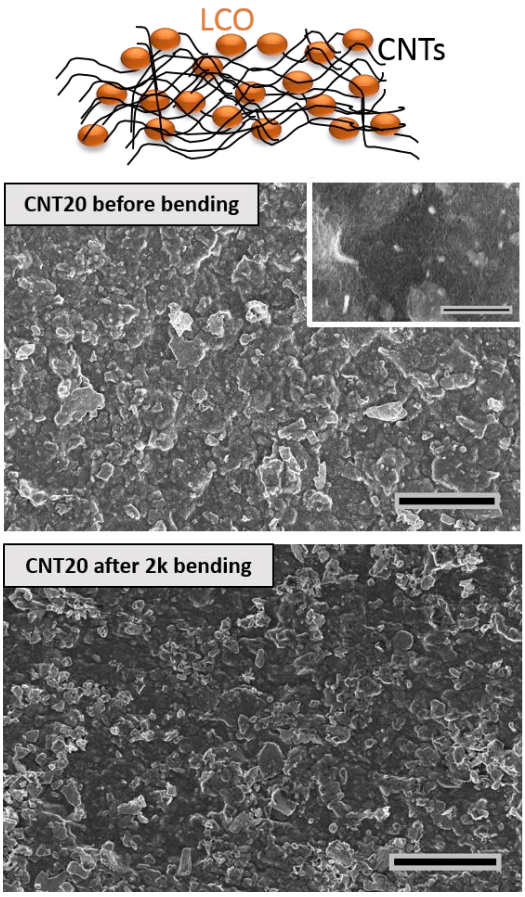

Figure S1: SEMs for the films with 20 wt% CNTs. Top row shows the films before bending, bottom row shows them after 2000 bending cycles. (Scale bar 50 µm, inset 2 µm).

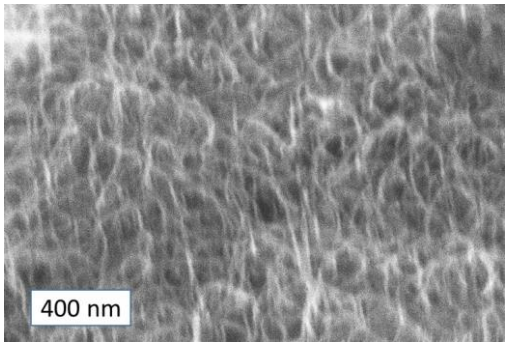

Figure S2: Close up SEM image of the CNT network in 10 wt% CNT films.

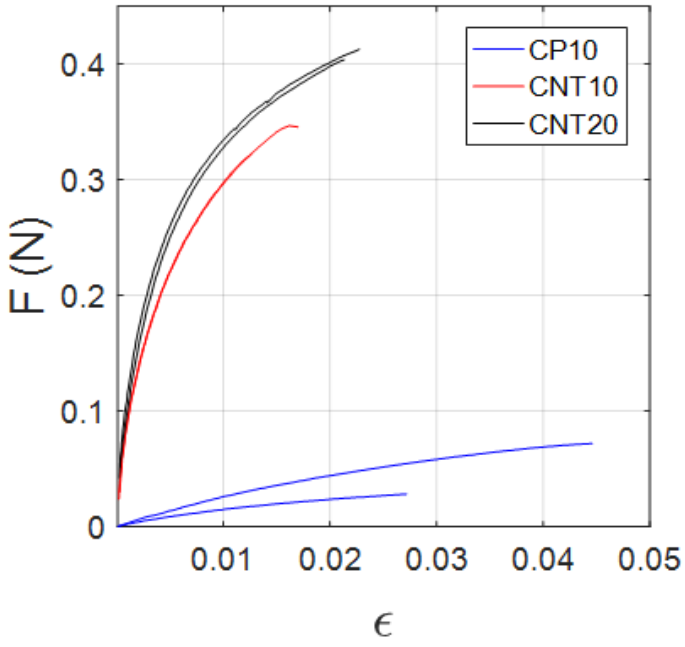

Figure S3: Force strain curves (2 measurements each) for the CNT10, CNT20 and CP10 films investigated.

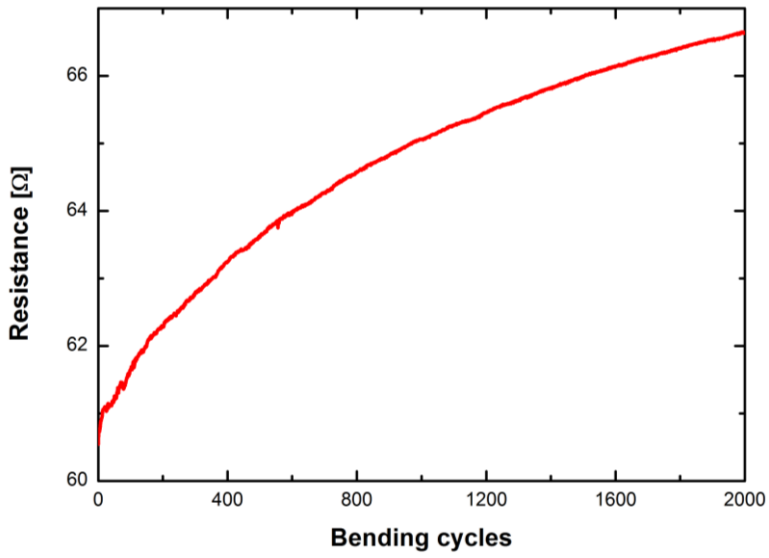

Figure S4: Resistance change with bending cycles for the CNT20 film.

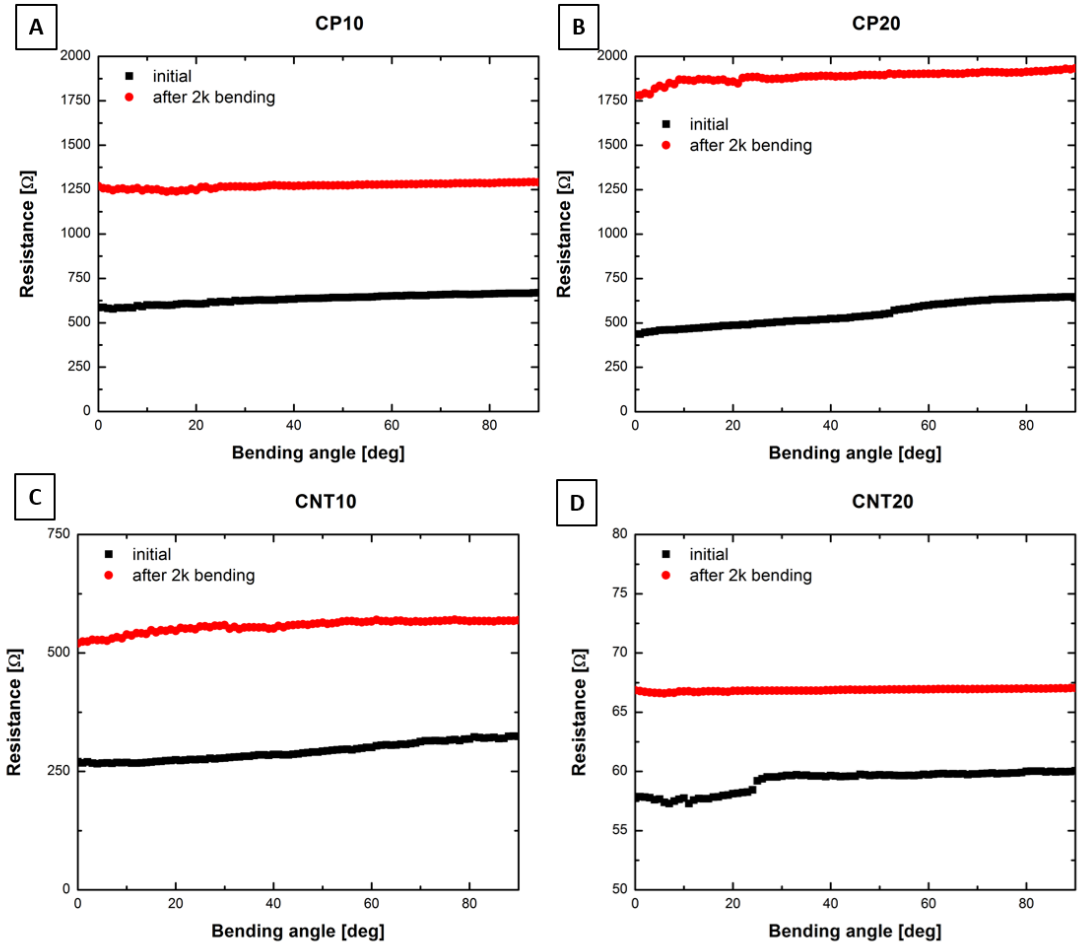

Figure S5: Comparison of the resistance for the different types of films, showing the large increase in initial resistance before and after 2000 bending cycles as well as the resistance change with the bending angle between 0º - 90º.